The *stumpy* gene is required for mammalian ciliogenesis

Terrence Town*†, Joshua J. Breunig‡, Matthew R. Sarkisian‡, Charalampos Spilianakis*§, Albert E. Ayoub‡, Xiuxin Liu‡, Anthony F. Ferrandino*, A. Rachel Gallagher¶, Ming O. Li*, Pasko Rakic‡, and Richard A. Flavell*§∥

Departments of *Immunobiology and ‡Neurobiology and Kavli Institute of Neuroscience, ¶Section of Nephrology, Department of Internal Medicine, and §Howard Hughes Medical Institute, Yale University School of Medicine, 300 Cedar Street, TAC S-569, New Haven, CT 06519-8011; and †Maxine Dunitz Neurosurgical Institute and Department of Biomedical Sciences, Cedars–Sinai Medical Center, 8700 Beverly Boulevard, Los Angeles, CA 90048

Contributed by Richard A. Flavell, January 7, 2008 (sent for review December 4, 2007)

Cilia are present on nearly all cell types in mammals and perform remarkably diverse functions. However, the mechanisms underlying ciliogenesis are unclear. Here, we cloned a previously uncharacterized highly conserved gene, *stumpy*, located on mouse chromosome 7. *Stumpy* was ubiquitously expressed, and conditional loss in mouse resulted in complete penetrance of perinatal hydrocephalus (HC) and severe polycystic kidney disease (PKD). We found that cilia in *stumpy* mutant brain and kidney cells were absent or markedly deformed, resulting in defective flow of cerebrospinal fluid. *Stumpy* colocalized with ciliary basal bodies, physically interacted with γ-tubulin, and was present along ciliary axonemes, suggesting that *stumpy* plays a role in ciliary axoneme extension. Therefore, *stumpy* is essential for ciliogenesis and may be involved in the pathogenesis of human congenital malformations such as HC and PKD.

brain | cilia | kidney | intraflagellar transport protein

Cilia are evolutionarily conserved organelles and are generally classified as primary (sensory, nonmotile) or motile [e.g., those expressed by ependymal cells in the brain that generate force necessary for cerebrospinal fluid (CSF) flow] (1, 2). The loss or defective function of cilia has been implicated in diseases such as obesity, diabetes, situs inversus, hydrocephalus (HC), and polycystic kidney disease (PKD) (3–8). The mechanisms regulating growth and stability of mammalian cilia during development are poorly understood. In attempting to explore the function of the transforming growth factor β1 gene (*tgfb1*) during development (9, 10), we established a conditional deficient mouse by inserting *loxP* sites 5′ of the promoter region of *tgfb1* and 3′ of *tgfb1* exon 1 (within the first intron). Importantly, during the generation of these mice, there were no known or predicted genes in close physical proximity to the *tgfb1* promoter region. However, a hypothetical gene (ENSMUSG00000063439) was later predicted in this region encoding cDNA sequence BC028440 (GenBank accession no. NM_172148) (11). We have termed this hypothetical gene *stumpy* as a result of experimental evidence presented here showing a key role of *stumpy* in the growth of primary and motile cilia.

Results

Establishment of Conditional *Stumpy* Mutant Mice and Expression Analysis. We deleted this genomic region in the brain by crossing floxed mice to *nestin-cre* deleter transgenic animals and determined deletion efficiency by PCR analysis of the floxed (but not deleted), deleted, or wild-type alleles (Fig. 1*A* and *Materials and Methods*). The deleted allele was most obviously detected in DNA prepared from brains of fl/fl mice but was undetectable in control +/+ animals (Fig. 1*B*). Remarkably, *stumpy* mRNA expression was dramatically reduced from 41.0- to 84.7-fold by Affymetrix GeneChip, whereas, unexpectedly, *tgfb1* mRNA expression was modestly (but significantly) increased by 1.8- to 3.0-fold in fl/fl vs. +/fl mice, raising the possibility of a *stumpy-tgfb1* read-through transcript created by the deleted allele (Fig.

1*C*). Three approaches were taken to test this hypothesis: donor splice/recipient bioinformatics, RT-PCR, and Northern blot. Bioinformatics predicted a chimeric in-frame readthrough transcript encoded by the deleted allele, comprised of exons 2–3 of *stumpy* and exons 2–7 of *tgfb1*. Complementary DNA was prepared from postnatal (P) day 12 brains of +/+, +/fl, or fl/fl mice, and RT-PCR was performed by using various primer combinations, which revealed the presence of a readthrough transcript in +/fl and fl/fl mice (Fig. 1*D*). Sequencing of this chimeric *stumpy-tgfb1* PCR product showed an in-frame transcript, and Northern blot analysis (Fig. 1*E*) further supported this conclusion. Therefore, we focused our efforts on characterizing the adjacent gene to determine whether this gene might underlie phenotypic defects present in these targeted mutant mice.

We initially characterized *stumpy* expression by quantitative real-time RT-PCR (Q-PCR, normalized to *hprt1* levels) by using cDNA prepared from organs of adult C57BL/6 mice, cultured Neuro-2a (N2a) neuroblastoma cells, or primary mouse microglia. *Stumpy* expression was widespread, with highest levels in mouse thymus and skeletal muscle, but we also detected expression in brain, N2a cells, and microglia (Fig. 1*F*). Using RNA *in situ* hybridization, we observed *stumpy* transcripts throughout the entire early postnatal brain, including cells lining the ventricles and Sylvian aqueduct (S. aq), and choroid plexus (C. Plexus) cells (Fig. 1*G*). To characterize *stumpy* mRNA, we then performed 5′- and 3′-RACE using cDNA prepared from adult C57BL/6 mouse brain, kidney, or liver. Interestingly, 5′-RACE revealed a noncoding exon 1 [supporting information (SI) Fig. 5 *A* and *B*], and 3′-RACE allowed for characterization of the 3′-UTR of *stumpy* mRNA (SI Fig. 5*C*). Bioinformatics analysis of *stumpy* mRNA (GenBank accession no. BC028440) revealed high conservation between vertebrate and invertebrate species (SI Fig. 6). SI Fig. 7*A* shows the complete coding sequence for *stumpy* (determined from RACE and cloning/sequencing analyses) with predicted translation indicated below (corresponding to hypothetical protein LOC232987, GenBank accession no. NP_742160) (11). Notably, protein family (*Pfam*) analysis revealed a B9/C2 calcium/lipid-binding region (*Pfam* references PF07162 and PF00168) spanning amino acids 4–106 (SI Fig. 7*B*). B9 is a highly conserved domain of unknown function present in 41 known or predicted eukaryotic proteins in both vertebrates and invertebrates (SI Fig. 8). The B9 domain is present in the ciliary proteome database (12), and a protein containing this
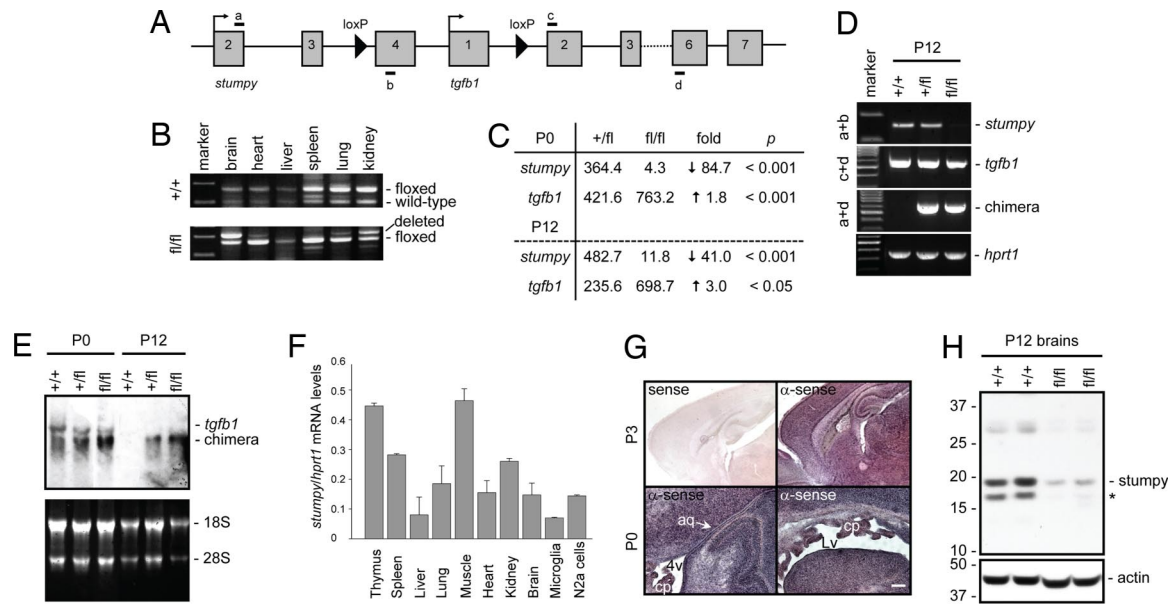
CELL BIOLOGY

Fig. 1. Generation of *stumpy* mutant mice and gene expression analysis. (*A*) Diagram showing insertion of *loxP* sites flanking exon 4 of *stumpy* and exon 1 of *tgfb1*. Positions of primers *a–d* used for RT-PCR or Northern blot probe are shown. (*B*) Multiplex PCR designed to detect floxed (but not deleted), deleted, or wild-type alleles at P0 from floxed but not deleted (+/+) or homozygous deleted (fl/fl) mice. (*C*) Affymetrix GeneChip results showing mRNA expression of *stumpy* or *tgfb1* in P0 and P12 brains from fl/fl vs. heterozygous (+/fl) mice. (*D*) RT-PCR using primer pairs shown in *A*. (*E*) Northern blot using a probe amplified from primers c and d shown in *A* reveals *tgfb1* or a chimeric *stumpy-tgfb1* in-frame read-through transcript in brains from fl/fl vs. +/fl mice. (*F*) Q-PCR analysis of *stumpy* relative to *hprt1* in mouse organs and cells. (*G*) RNA *in situ* hybridization with *stumpy* α-sense or sense (control) probes in wild-type C57BL/6 mouse brains. Higher-magnification images (*Lower*, scale bar denotes 50 μm, calculated for *Lower Left* and *Lower Right*) reveal expression in cells lining the 4v, the S. aq, Lv, and in C. Plexus (cp). (*H*) Brain homogenates from P12 +/+ or fl/fl mice were Western blotted with stumpy antibody (*Upper*). Note the ≈19-kDa band corresponding to the predicted molecular mass for stumpy. ∗ shows a possible stumpy degraded product, and actin is shown *Lower* as a loading control.

domain, MKS1, has recently been linked to ciliogenesis (13). To confirm stumpy deficiency at the protein level, we generated a stumpy antibody and probed brain homogenates from +/+ and fl/fl mice. We noted the presence of a ≈19-kDa band, corresponding to the predicted molecular mass of stumpy, which was nearly absent in conditional *stumpy* deficient mice (Fig. 1*H*).

Perinatal HC and PKD in Conditional *Stumpy* Mutant Mice. Upon gross anatomical observation, it was readily apparent that homozygous fl/fl *stumpy* mutant mice had a "domed" head that became prominent from P12 to P16, and was not observed in heterozygous (+/fl) animals (Fig. 2*A*). This phenotype suggested the presence of HC, a condition that results from cerebral ventricle dilation secondary to altered flow of CSF (14). Consistently, we found that fl/fl mice displayed an enlarged, balloon-like and translucent neocortex (nctx) by P16 (Fig. 2*B*). H&E staining of coronal brain sections revealed pronounced ventricular enlargement in fl/fl mice (Fig. 2*B*). Also at this age, bodies of *stumpy* fl/fl mice weighed significantly less than littermate controls, whereas their brains weighed more (likely because of increased CSF volume) (*n* = 7 for +/+, *n* = 10 for +/fl, and *n* = 6 for fl/fl; mean weights in grams ± SE, brain: 0.39 ± 0.02, 0.39 ± 0.02, 0.52 ± 0.04, *P* < 0.001; body: 7.59 ± 0.15, 7.14 ± 0.74, 4.34 ± 0.63, *P* < 0.001). Crosses of *stumpy* mutant mice heterozygous for the floxed allele and either positive (cre +, +/fl) or negative (cre−, +/fl) for the *nestin-cre* transgene yielded numbers for each genotype of observed (obs) offspring that did not significantly differ from expected (exp) Mendelian frequencies ($\chi^2_{(5)}$ = 5.48, *P* = 0.36) (Fig. 2*C*), suggesting that fl/fl mice were not being lost due to embryonic lethality. Notably, perinatal HC occurred with complete penetrance in homozygous *stumpy* mutant mice (fl/fl, designated cre +, fl/fl in Fig. 2*C*). All of the hydrocephalic animals in this study died by the time of weaning (P21).

Two control pups developed the disease, which may represent spontaneous incidence of hydrocephaly in C57BL/6 mice (<1%) (15). We used an important control mouse group in our analyses (+/fl mice, heterozygous for the *nestin-cre* transgene) to rule out *cre*-mediated effects in fl/fl mice (heterozygous for the *nestin-cre* transgene and homozygous for the floxed allele), given that mice homozygous for this transgene develop microencephaly and hydrocephalus (16). We did not observe any incidence of HC in +/fl mice.

Congenital HC in mice (and in humans) can be attributed to blockage of CSF flow, a failure in CSF absorption, or overproduction of CSF (15). Histological analysis of brains from +/fl vs. fl/fl mice at P1 (but not at P0) revealed stenosis of the mesencephalic S. aq (which joins the third and fourth ventricles) in fl/fl mice before the onset of ventriculomegaly (Fig. 2*D*). By P16, the S. aq remained stenotic in fl/fl mice and was accompanied by marked third ventricle (3v) and lateral ventricle (Lv) enlargement, producing a thinner neocortex (Fig. 2*D*). These pathological changes were consistent with a form of communicating HC known as perinatal triventricular HC (PTvHC) characterized by another group in axonemal dynein heavy chain gene *mdnah5* mutant mice (3). PTvHC in fl/fl mice was associated with tonic seizures and severe motor dysfunction (data not shown), and behavioral assay of motor function at P16 revealed significant (*P* < 0.001) impairment in fl/fl mice in an accelerating rotating rod apparatus (Fig. 2*E*). In addition to efficiently recombining cre/loxP in the central nervous system, *nestin-cre* transgenic mice also delete floxed alleles in the kidney (17). Accordingly, we noted *stumpy* deletion in the kidney (Fig. 1*B*), which prompted us to examine kidney sections by H&E histochemistry. Strikingly, all of the fl/fl mice examined had prominent evidence of PKD (Fig. 2*F*). Confocal microscopy with lectins lotus tetragonolobus agglutinin and dolichos biflorus agglutinin revealed that both proximal and distal segments of the nephron were cystic in fl/fl mice (data not shown).

Fig. 2. PTvHC communicating HC and polycystic kidney disease in *stumpy* mutant mice. (*A*) Photographs of representative +/fl and fl/fl mice (*Upper*) showing classic ''domed head'' of hydrocephalic fl/fl mice at P16. By P12, fl/fl mice consistently appear runted (*Lower*). (*B*) Whole brains isolated from +/fl and fl/fl mice (*Left*), and low-magnification photomicrographs of H&E-stained coronal brain sections (*Right*) showing pronounced venticulomegaly. (*C*) *Nestin-cre*-positive mice bearing one floxed allele (cre +, +/fl) were crossed with *nestin-cre*-negative –, +/fl mice, and all deficient offspring (cre +, fl/fl) manifested perinatal hydrocephaly. An additional 20/104 hydrocephalic cre +, fl/fl mice were identified from cre +, +/fl x cre–, fl/fl breedings. (*D*) Coronal H&E-stained sections show complete stenosis of the S. aq in fl/fl brains (*Right*). An enlarged 3v and thinner neocortex (nctx) are also observed in fl/fl brains (*Right*). (Scale bars, 100 μm.) (*E*) Motor function in wild-type (+/+, n = 9), +/fl (n = 10), and fl/fl mice (n = 6) was assayed by accelerating roto-rod, and data are represented as means ± SE of time to fall (latency, in seconds) for each of three consecutive trials. *, $P < 0.001$ for fl/fl vs. +/fl or +/+. (*F*) H&E-stained sections from +/fl or fl/fl P12 kidneys show evidence of polycystic kidney disease. High-magnification *Insets* are shown in the upper right corners. (Scale bars, 20 μm.)

Stumpy Conditional Mutant Mice Lack Functional Intact Cilia.

We hypothesized that HC in conditional *stumpy* mutant mice might be due to a defect in the ependymal cell layer that regulates CSF flow. High magnification of H&E-stained brain sections from fl/fl vs. +/fl mice revealed that ependymal cells in the 3v appeared dysmorphic but apparently intact (Fig. 3*A*). More notably, we observed that cilia on ependymal cells lining the S. aq and the cerebral ventricles (3v is shown, similar results were observed in the Lv and 4v) were nearly absent in fl/fl mice (Fig. 3*A*). This observation suggests that *stumpy* may be implicated in

Fig. 3. Ciliogenesis defects in *stumpy* mutant mice. (*A*) P16 +/fl or fl/fl H&E-stained sections showing the S. aq (*Upper*) and the ependyma of 3v (*Lower*). Arrowheads indicate cilia. (Scale bars, 20 μm.) (*B*) Vibratome brain sections from the F. Monroe (*Top*) or cryosections from 4v or the C. Plexus from +/fl (*Left*) or fl/fl mice (*Right*) at P4 were immunostained for acetylated α-tubulin (against the ciliary axoneme), rootletin (against ciliary rootlets), and/or γ-tubulin (recognizes ciliary bb) (colors for each antibody are indicated), and nuclear counterstained with DAPI (blue). Images were captured by using a Zeiss ApoTome-equipped fluorescence microscope (*Top*) or a confocal microscope (all other images). Arrowheads in the C. Plexus show ciliary axonemes. (Scale bars, 10 μm.) (*C*) Transmission electron micrographs of cells lining the S. aq are shown from P0 +/fl (*Left*) or fl/fl mice (*Right* and *Bottom*). Higher magnifications of *Insets* (*Top*) are shown below in *Middle* (*Middle Insets* show additional examples). Note the presence of bb structures in both +/fl and fl/fl mice, whereas fl/fl cells either do not have ciliary axonemes (c) or they appear deformed. *Bottom* show serial EM sections (0–420 nm) through bb structures of the boxed region, demonstrating the absence of c structures in a mutant S. aq cell. [Scale bars: *Top*, 2 μm; *Middle* and *Bottom*, 0.5 μm.] (*D*) Confocal microscopy was performed on kidneys isolated from P12 +/fl or fl/fl mice after α-tubulin immunostaining. Arrowheads indicate cilia. (Scale bars, 20 μm.)

ciliogenesis. Indeed, *stumpy* fl/fl mutants had dramatically fewer motile cilia (as detected by antibody against acetyl α-tubulin, a major structural component of ciliary axonemes) (18–20) in the foramen of Monroe (F. Monroe) and in the fourth ventricle (4v; similar findings were made in the Lv and 3v) (Fig. 3*B*). Ciliary axonemes that were present in fl/fl mice had a "stumpy-like" appearance. Interestingly, ciliary rootlets (at the ciliary base, detected by rootletin antibody) (21) appeared normal in cells lining the CSF system of +/fl and fl/fl mice (Fig. 3*B*). Similar results were observed for primary cilia on C. Plexus cells; specifically, acetyl α-tubulin antibody-positive ciliary axonemes were almost completely absent, whereas ciliary basal bodies (bb, another anchoring component of cilia, detected by γ-tubulin antibody) (22) or rootletin-positivity was comparable between P4 fl/fl and +/fl brains (Fig. 3*B*). Electron microscopy analysis revealed numerous intact bb structures in the S. aq of P0 fl/fl mice; however, cells lining the ventricles either completely lacked proper ciliary axonemal extensions, or had markedly deformed structures (Fig. 3*C*). Although +/fl mice displayed
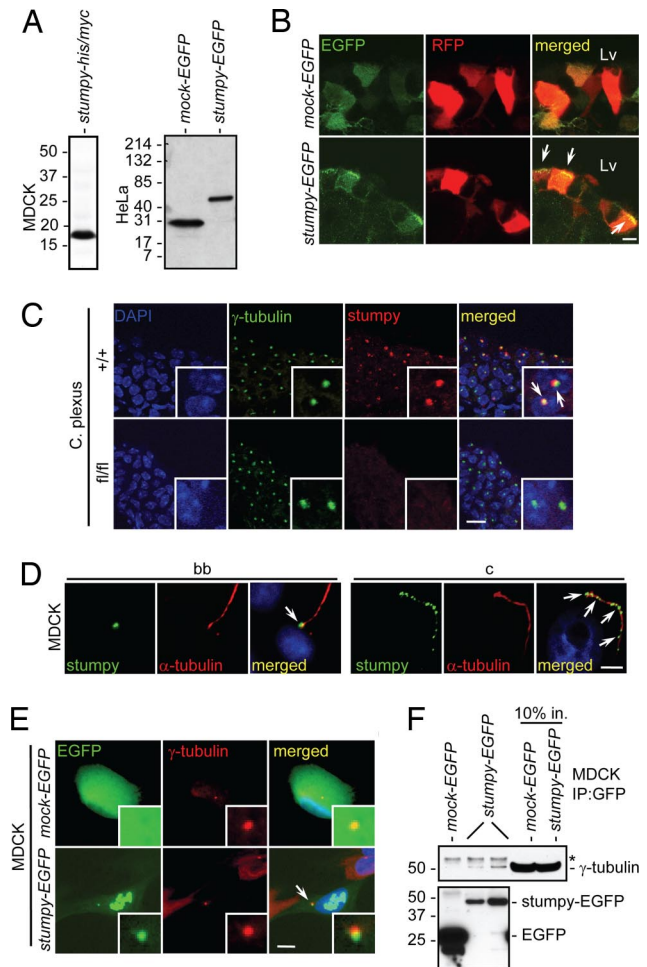
CELL BIOLOGY

robust cilia, serial sectioning confirmed the lack of axonemal protrusion from bb structures in the fl/fl mouse (Fig. 3C). Recent evidence has shown that defective cilia lead to kidney cyst formation (6), leading us to examine cilia on kidney tubule cells. We noted a pattern of results similar to what we observed in the brain: ciliary axonemes in fl/fl mice were either completely absent or, when present, often had a "stumpy" appearance (Fig. 3D).

We tested whether cilia beating frequency was altered in fl/fl mice vs. +/fl littermate controls by using an electrophysiological technique. Although generally difficult to detect ciliary movement in the S. aq of fl/fl mice (i.e., we observed a flat line), likely due to the widespread loss of cilia, beating frequency of remaining cilia was not significantly different in fl/+ vs. fl/fl mice (number, mean ± SD for fl/+ vs. fl/fl mice: $n = 5$, $12.8 ± 2.2$ Hz vs. $n = 3$, $10.9 ± 1.2$ Hz, $P > 0.05$) (SI Fig. 9). The presence of few cilia may be due to incomplete deletion in a small fraction of conditional *stumpy* mutant cells, and suggests that *stumpy* may be required more for growth (ciliogenesis) rather than function *per se*. Finally, we assayed CSF flow in +/fl vs. fl/fl mice by acutely injecting India Ink (as a tracer) into the CSF system of live brain slices and monitored flow by real-time video microscopy. This analysis revealed a profound defect in CSF flow in fl/fl mice (SI Movie 1). Thus, *stumpy* appears to be essential for cilia outgrowth, the lack of which results in failure of CSF flow.

Defective Ciliogenesis in *Stumpy* Conditional Mutant Mice Is *tgfb1* Independent. Conditional *stumpy* mutants lack exon 4 of *stumpy* and exon 1 of *tgfb1* (Fig. 1), resulting in generation of a chimeric, in-frame *stumpy-tgfb1* readthrough mRNA transcript. To determine whether deficiency in *tgfb1* exon 1 contributed to the ciliogenesis defect and HC observed in fl/fl mice, we crossed heterozygous (+/fl) *stumpy* mutant mice with another mouse that is heterozygous for *egfp* knocked-in to exon 1 of *tgfb1*, resulting in a null *tgfb1* frame-shift mutation (progeny heterozygous for both alleles are designated +/fl/tgfb1egfp^KI+; see SI Fig. 10A for a diagram). These mice did not manifest HC, and had normal ciliogenesis in ependymal cells lining the ventricles and the C. Plexus (SI Fig. 10A). Alternatively, the defects in conditional *stumpy* mutants could be owed to a gain of (dys) function of the *stumpy-tgfb1* chimera. To test this, we cloned the *stumpy* complete coding sequence into an adenovirus with a bicistronic EGFP reporter (pAdTrack) (23). We then intracerebroventricularly (i.c.v.) injected embryonic day 14.5 fl/fl embryos with adenovirus and analyzed their brains at P12. The adenovirus predominantly infected C. Plexus cells (SI Fig. 10B). Remarkably, we observed that EGFP-positive cells clearly had multiple detectable α-tubulin-positive ciliary axonemes, whereas surrounding EGFP-negative cells lacked these structures, or they appeared "stumpy" (SI Fig. 10B). Finally, we evaluated mice conditionally deficient in brain TGF-β receptor II (required for TGF-β signaling, obtained by crossing TGF-β receptor II floxed mice with *nestin-cre* transgenics), and these animals appear normal without incidence of hydrocephaly (data not shown). Together, these data suggest that neither *tgfb1* (signaling) deficiency nor *stumpy-tgfb1* chimerism underlies the phenotype, and that *stumpy* deficiency is responsible for both the cilogenesis defect and HC.

Stumpy Localizes to the Ciliary-bb and Physically Interacts with γ-Tubulin. To gain insight into the function and localization of stumpy, we first generated either poly-*histidine*/poly-*myc* (*his/myc*) or *EGFP*-tagged *stumpy* constructs and transiently transfected canine kidney epithelial (MDCK) or human cervical cancer (HeLa) cells. Western blots of transfectants with myc or GFP antibodies revealed that stumpy protein was ≈19 kDa (Fig. 4A), consistent with Western blot of mouse brain homogenates with stumpy antibody (Fig. 1H). We then coelectroporated

Fig. 4. *Stumpy* is an essential component of the ciliary bb and axoneme. (A) MDCK (*Left*) or HeLa (*Right*) cells were transiently transfected with *stumpy-his/myc*, *mock-EGFP*, or *stumpy-EGFP* plasmids. After 48 h, cell lysates were Western blotted with anti-myc or GFP antibodies. (B) Embryonic day 15 fetuses were coelectroporated with plasmids encoding *RFP* and *mock-EGFP* or *stumpy-EGFP*. RFP+ ependymal cells along Lv were imaged at P10. Arrowheads show apical localization of *stumpy*-EGFP compared with diffuse EGFP signal in Mock-transfected cells. (Scale bar, 5 μm.) (C) C. Plexus +/+ or fl/fl mice was immunostained for γ-tubulin (green signal) and *stumpy* (red signal) (arrowheads show colocalization; high-magnification *Insets* are in the bottom right). (Scale bar, 20 μm.) (D) Differentiated MDCK cells were immunostained for stumpy (green signal) or α-tubulin (red signal) (merged images are shown to the right). (Scale bar, 5 μm.) Note *stumpy* signal at the bb (*Left*, see arrowhead) and ciliary axoneme (c) (*Right*; see arrowheads). MDCK cells were stably transfected with *mock-EGFP* or *stumpy-EGFP* plasmids (green signal), and (E) immunostained with γ-tubulin (red signal) (merged images are shown to the right; arrowhead shows colocalized signals; high-magnification *Insets* are in the bottom right) (scale bar, 5 μm) or (F) cell lysates were immunoprecipitated with GFP antibody and Western blotted with γ-tubulin (*Upper*) or GFP antibody (*Lower*). Ten percent input controls are shown to the right, and * indicates rabbit Ig heavy chain. For *C–E*, DAPI was used as a nuclear counterstain (blue signal). Images were captured by using a confocal microscope (*B* and *C*), a Zeiss ApoTome-equipped fluorescence microscope (*D*), or an epifluorescence microscope (*E*).

mouse fetus brain Lvs with *red fluorescence protein* (*RFP*) and *mock-EGFP* or *stumpy-EGFP* constructs and imaged Lv ependymal cells by confocal microscopy. We observed that stumpy-EGFP (but not mock-EGFP) localized to the apical surface of RFP-positive ependymal cells, reminiscent of ciliary bb structures (Fig. 4B). To directly assess whether stumpy localized to the bb, we immunostained brains from +/+ or fl/fl mice with

γ-tubulin and stumpy antibodies. We found colocalization of these proteins in ependymal cells (data not shown) and in C. Plexus (Fig. 4C). Consistently, MDCK cells showed stumpy signal at the base of α-tubulin-positive ciliary axonemes by immunostaining (Fig. 4D). Further, we observed a punctate pattern of stumpy immunoreactivity along ciliary axonemes (Fig. 4D). To further confirm γ-tubulin colocalization and to test for putative physical interaction between stumpy and γ-tubulin, we generated MDCK cell lines stably expressing *stumpy-EGFP* or *mock-EGFP* constructs and performed immunofluorescence microscopy and coimmunoprecipitation assays. Stumpy colocalized with γ-tubulin, and could also be observed in euchromatic regions of the nucleus (Fig. 4E). Further, pull-down with GFP antibody coimmunoprecipitated γ-tubulin in *stumpy-EGFP* but not *mock-EGFP* MDCK transfectants (Fig. 4F). These results suggest that stumpy is a critical component of the ciliary bb and axoneme.

Discussion

Here, we present evidence that *stumpy* mutant mice have a profound defect in ciliogenesis associated with complete penetrance of PTvHC and PKD. A causal relationship between disturbed CSF flow homeostasis (brought on by dysfunctional cilia) and HC has been suggested by others (3–5). This may be due to poor CSF flow resulting from dysfunction of motile cilia on ependymal cells or failure of primary cilia on C. Plexus cells, which are thought to be important regulators of CSF production (4). Ciliogenesis has been suggested to be calcium-dependent (24), and it is noteworthy that another B9/C2 calcium/lipid-binding domain-containing protein, MKS1, has recently been localized to the ciliary bb (25). Mutation in this gene has recently been linked to Meckel Syndrome, a severe fetal developmental disorder hallmarked by occipital meningoencephalocele, cystic kidney dysplasia, fibrotic changes of the liver, and polydactyly (13). *Stumpy* appears to have a general role in ciliogenesis, because we show that *stumpy* mutant mice also have PKD and striking loss of cilia on nephron epithelial cells. Interestingly, our results show that the *nestin-cre* deleter mice are able to recombine in the kidney when crossed with *stumpy* floxed mice, consistent with recent reports showing nestin expression in human kidney and recombination of kidney cells in *nestin-cre* mice (17, 26). This should be a consideration for the neuroscientist who is interested in only recombining brain cells and is considering using *nestin-cre* deleter mice. Consistent with our findings in mammals, another group has shown that knocking down the *stumpy* ortholog in paramecium using RNA interference results in loss of cilia stability (27).

Interestingly, *stumpy* is atypical in that it is located in tight physical proximity to the *tgfb1* gene, and conditional stumpy mutant mice lack *stumpy* exon 4 and *tgfb1* exon 1. To determine how *tgfb1* deficiency impacted the phenotype of *stumpy* mutant mice, we took two approaches: (*i*) crossed heterozygous *stumpy* mutant mice with mice heterozygous for a null *tgfb1* allele, and (*ii*) i.c.v. delivered *stumpy* cDNA in pAdTrack adenovirus into fetuses of *stumpy* mutant mice or control littermates. Progeny from the crossing strategy homozygously deficient for *tgfb1* but heterozygous for *stumpy* were essentially normal. When we reintroduced *stumpy* into brains of conditional *stumpy* mutant mice by adenoviral delivery, we noted that infected C. Plexus cells had intact cilia, whereas neighboring noninfected cells did not. Taken together, these results support that *stumpy* deficiency as opposed to loss of *tgfb1* is responsible for defective ciliogenesis.

Stumpy is critical for the proper elongation of cilia. Although the precise biochemical nature of its function requires further investigation, the presence of stumpy within ciliary axonemes suggests it could associate with intraflagellar transport proteins (IFTs), large proteins that orchestrate bidirectional movement of substances within cilia and are required for steady-state assembly of tubulin onto the distal end of the ciliary axoneme (2). Our observation of stumpy localization at the ciliary bb further suggests an IFT role for this molecule. Strikingly, we find complete penetrance of both PTvHC and PKD in *stumpy* mutant mice, suggesting a general role for *stumpy* in mammalian ciliogenesis. We hypothesize that mutations in the highly conserved human homolog of this gene (MGC4093, located on chromosome 19 in close proximity to *tgfb1*, GenBank accession no. NM_030578) may be linked to congenital HC, PKD, and/or other developmental defects associated with abnormal cilia growth in humans. Such findings would serve to further highlight the role of previously underappreciated mammalian cilia in both physiological and disease processes.

Materials and Methods

Mice. Conditional *stumpy* mutant mice were established by inserting one *loxP* site in the intronic region just upstream of the last exon of *stumpy* and another *loxP* sequence in the intronic region between exons 1 and 2 of *tgfb1* (28). Additional mice were established with an *egfp* sequence ''knocked-in'' in place of exon 1 of *tgfb1* (designated *tgfb1egfp^{KI+}*), resulting in a null frameshift mutation in *tgfb1* (M.O.L and R.A.F., unpublished work). Both of these mice were bred with transgenic *nestin-cre* mice [B6.Cg-Tg(Nes-cre)1Kln/J] (29) obtained from The Jackson Laboratory. We examined >300 mice over a 3-year period in this study. All of the mice used in this study were fully backcrossed onto a C57BL/6 background.

Histochemistry and Light Microscopy. Postnatal mice (from P0 to P16) were perfused with ice-cold PBS, and brains and kidneys were rapidly isolated. Brains were dissected down the midline (for sagittal sectioning) or at the level of the anterior commissure (for coronal sectioning) using a mouse brain slicer (World Precision Instruments); kidneys were dissected down the midline. Cerebral pieces were immersion-fixed in 4% PFA overnight at 4°C. For H&E histochemistry, cerebral pieces were routinely embedded in paraffin for microtome sectioning at 8-μm thickness, applied to Superfrost Plus Gold slides (Fisher Scientific), deparaffinized in xylene, hydrated in a graded series of ethanols, and stained with H&E Y (Sigma) according to standard practice. Stained sections were dehydrated and mounted in Permount (Fisher Scientific), air-dried, and viewed by using an automated Olympus BX-61 microscope with attached Olympus MagnaFire CCD imaging system. See *SI Text* for more methodological details.

1. Porter ME, Sale WS (2000) The 9 + 2 axoneme anchors multiple inner arm dyneins and a network of kinases and phosphatases that control motility. *J Cell Biol* 151:F37–F42.
2. Davenport JR, Yoder BK (2005) An incredible decade for the primary cilium: a look at a once-forgotten organelle. *Am J Physiol* 289:F1159–F1169.
3. Ibanez-Tallon I, et al. (2004) Dysfunction of axonemal dynein heavy chain Mdnah5 inhibits ependymal flow and reveals a novel mechanism for hydrocephalus formation. *Hum Mol Genet* 13:2133–2141.
4. Banizs B, et al. (2005) Dysfunctional cilia lead to altered ependyma and choroid plexus function, and result in the formation of hydrocephalus. *Development* 132:5329–5339.
5. Sawamoto K, et al. (2006) New neurons follow the flow of cerebrospinal fluid in the adult brain. *Science* 311:629–632.
6. Yoder BK (2007) Role of primary cilia in the pathogenesis of polycystic kidney disease. *J Am Soc Nephrol* 18:1381–1388.
7. Davenport JR, et al. (2007) Disruption of intraflagellar transport in adult mice leads to obesity and slow-onset cystic kidney disease. *Curr Biol* 17:1586–1594.
8. Ainsworth C (2007) Cilia: tails of the unexpected. *Nature* 448:638–641.
9. Pintavorn P, Ballermann BJ (1997) TGF-beta and the endothelium during immune injury. *Kidney Int* 51:1401–1412.

10. Li MO, Wan YY, Sanjabi S, Robertson AK, Flavell RA (2006) Transforming Growth Factor-beta Regulation of Immune Responses. *Annu Rev Immunol* 24:99–146.

11. Katayama S, *et al.* (2005) Antisense transcription in the mammalian transcriptome. *Science* 309:1564–1566.

12. Gherman A, Davis EE, Katsanis N (2006) The ciliary proteome database: an integrated community resource for the genetic and functional dissection of cilia. *Nat Genet* 38:961–962.

13. Kyttala M, *et al.* (2006) MKS1, encoding a component of the flagellar apparatus basal body proteome, is mutated in Meckel syndrome. *Nat Genet* 38:155–157.

14. Bruni JE, Del Bigio MR, Cardoso ER, Persaud TV (1988) Hereditary hydrocephalus in laboratory animals and humans. *Exp Pathol* 35:239–246.

15. The Jackson Laboratory (2003) *Hydrocephalus in Laboratory Mice*, http://jaxmice.jax.org/library/notes/490f.html.

16. Forni PE, *et al.* (2006) High levels of Cre expression in neuronal progenitors cause defects in brain development leading to microencephaly and hydrocephaly. *J Neurosci* 26:9593–9602.

17. Dubois NC, Hofmann D, Kaloulis K, Bishop JM, Trumpp A (2006) Nestin-Cre transgenic mouse line Nes-Cre1 mediates highly efficient Cre/loxP mediated recombination in the nervous system, kidney, and somite-derived tissues. *Genesis* 44:355–360.

18. Piperno G, LeDizet M, Chang XJ (1987) Microtubules containing acetylated alpha-tubulin in mammalian cells in culture. *J Cell Biol* 104:289–302.

19. LeDizet M, Piperno G (1987) Identification of an acetylation site of Chlamydomonas alpha-tubulin. *Proc Natl Acad Sci USA* 84:5720–5724.

20. LeDizet M, Piperno G (1991) Detection of acetylated alpha-tubulin by specific antibodies. *Methods Enzymol* 196:264–274.

21. Yang J, *et al.* (2002) Rootletin, a novel coiled-coil protein, is a structural component of the ciliary rootlet. *J Cell Biol* 159:431–440.

22. Oakley BR (1992) Gamma-tubulin: the microtubule organizer? *Trends Cell Biol* 2:1–5.

23. He TC, *et al.* (1998) A simplified system for generating recombinant adenoviruses. *Proc Natl Acad Sci USA* 95:2509–2514.

24. Ueno H, Gonda K, Takeda T, Numata O (2003) Identification of elongation factor-1alpha as a Ca2+/calmodulin-binding protein in Tetrahymena cilia. *Cell Motil Cytoskeleton* 55:51–60.

25. Dawe HR, *et al.* (2007) The Meckel-Gruber Syndrome proteins MKS1 and meckelin interact and are required for primary cilium formation. *Hum Mol Genet* 16:173–186.

26. Perry J, *et al.* (2007) The intermediate filament nestin is highly expressed in normal human podocytes and podocytes in glomerular disease. *Pediatr Dev Pathol* 10:369–382.

27. Ponsard C, *et al.* (2007) Identification of ICIS-1, a new protein involved in cilia stability. *Front Biosci* 12:1661–1669.

28. Li MO, Wan YY, Flavell RA (2007) T cell-produced transforming growth factor-beta1 controls T cell tolerance and regulates Th1- and Th17-cell differentiation. *Immunity* 26:579–591.

29. Tronche F, *et al.* (1999) Disruption of the glucocorticoid receptor gene in the nervous system results in reduced anxiety. *Nat Genet* 23:99–103.